Introduction

The pressure wavefield recorded by a horizontal or slanted streamer in the presence of a calm sea surface can be directly de-ghosted in a spectral domain. Horizontal and slanted de-ghosting algorithms are therefore computationally efficient, and in case of mild variations this restrictive assumption on streamer shape can be accommodated for by optimizing the ghost model parameters in time-space windows.

Recently, variable-depth and rough sea-surface de-ghosting emerged as feasible and useful broadband processing steps (King et al. 2015, Hardwick et al. 2015). When changes in sea surface or receiver depth occur over short spatial distances, the de-ghosting problem can be formulated as a linear system of equations in the unknown up-going pressure wavefield. The fundamental building blocks of these equations are phase-shift redatuming operators that relate wavefields at different non-horizontal datums within the water column, for a constant or depth-varying water velocity profile. We therefore name this algorithm phase-shift de-ghosting.

Phase-shift de-ghosting

Pressure recorded along the streamer cable c at a certain termporal frequency ω and spatial location $\mathbf{x}$ is composed of an upgoing and a down-going part:

$$\mathbf{p}_c(\mathbf{x}) = \mathbf{u}_c + \mathbf{d}_c \qquad (1)$$

If receivers are placed at arbitrary depths the spatial Fourier transform of the recorded wavefield gives a distorted representation of its wavenumbers. It is therefore necessary to pose the de-ghosting problem as estimation of the wavenumber components of the up-going wavefield $\mathbf{u}_0(\mathbf{k})$ on a convenient horizontal datum, here taken to be at mean sea level. Wavefield $\mathbf{u}_c(\mathbf{x})$ is related to $\mathbf{u}_0(\mathbf{k})$ by the joint re-datuming and spatial reverse transform operator $\mathbf{W}_{0c}^-$:

$$\mathbf{u}_c = \mathbf{W}_{0c}^- \mathbf{u}_0$$

Similarly, the down-going part is: $\qquad\qquad (2),$

$$\mathbf{d}_c = r\mathbf{W}_{sc}^+ \mathbf{W}_{0s}^- \mathbf{u}_0$$

where $\mathbf{W}_{0s}^-$ and $\mathbf{W}_{sc}^+$ are the re-datuming operators from mean sea level to rough sea-surface and from rough sea-surface to streamer cable, respectively, and r is the frequency-dependent sea-surface reflectivity. In this notation, a '+' refers to the re-datuming of the down-going wavefield while a '-' is for the up-going. Substitution of (2) into (1) gives

$$\mathbf{p}_c(\mathbf{x}) = [\mathbf{W}_{0c}^- + r\mathbf{W}_{sc}^+ \mathbf{W}_{0s}^-]\mathbf{u}_0(\mathbf{k}) = \mathbf{G}\mathbf{u}_0(\mathbf{k}) \qquad (3).$$

The $\mathbf{W}$ operators in (3) can be defined for variable water velocity and rough sea, as well as for an arbitrary cable profile. Using (3), the de-ghosting problem is solved as

$$\mathbf{u}_0 = \mathbf{G}^{-1}\mathbf{p}_c \ (4),$$

and requires the inversion of $\mathbf{G}$. For each frequency of interest, we invert $\mathbf{G}$ using the LSQR algorithm of Paige and Saunders (1982), and we make use of a pyramid scheme that spatially down samples individual frequencies to their spatial Nyquist in order to reduce computational cost.

In the case of a calm sea-surface (s=0) the $\mathbf{d}_c$ expression in (2) can be simplified by re-datuming to the mirror receiver location, and therefore $\mathbf{d}_c = r\mathbf{W}_{0c}^+ \mathbf{u}_0$. In this particular case, and if, additionally, the water velocity is constant, operator $\mathbf{G}$ defines the f-k de-ghosting linear system of equations of Riyanti et al. (2008), later formulated in the τ-p domain by Poole (2013). King and Poole (2015)

discuss the rough-sea pressure de-ghosting problem and propose a solution that makes use of the sea-surface elevation while assuming mirror receivers.

Information relating to the cable depth and water velocity are routinely acquired during a survey and the sea-surface profile may be measured or estimated at each channel location, for example, by methods discussed in Kragh et al. (2004) and Hardwick et al. (2015). In our experience it is possible to estimate a sea surface profile from the frequency location of ghost notches in the *ω-x* domain, after taking into account the natural variation of the ghost-period with offset induced by the cable shape. If a time-variant sea surface profile is required, estimation and de-ghosting can take place in time windows. A Kurtosis-based approach can then be used to optimize the receiver depths when required (Grion et al. 2015)
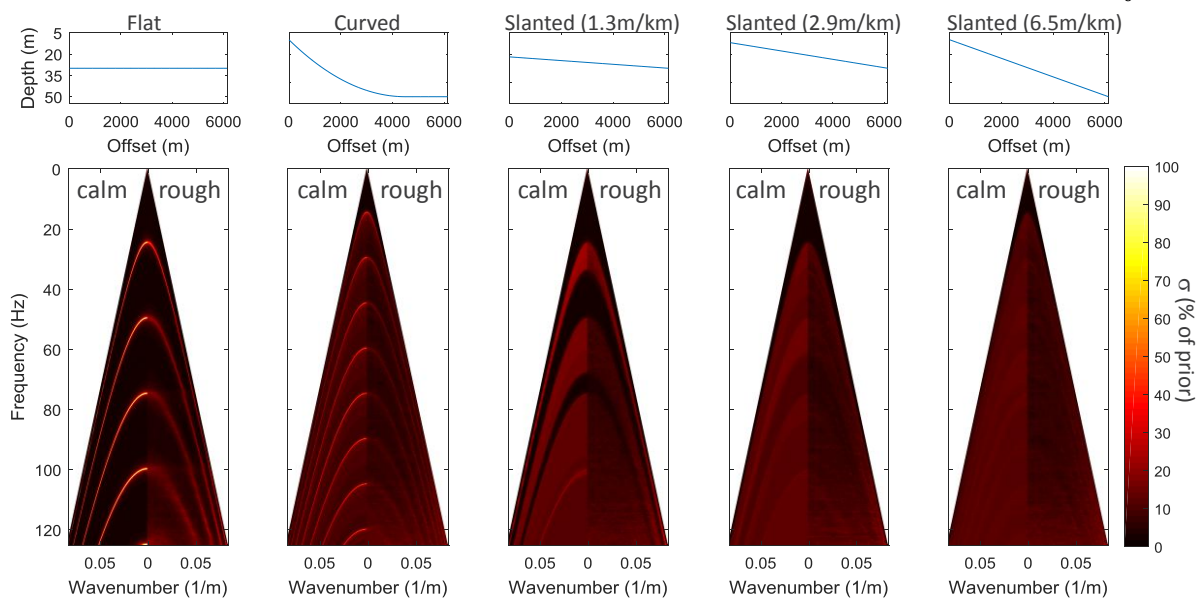
De-ghosting posterior covariance

The formulation of de-ghosting as an inverse problem allows the calculation of *posterior* covariances based on assumptions on *prior* total and up-going pressure uncertainties. Assuming prior Gaussian uncertainties characterized by covariance matrices $\mathbf{C}_{\mathbf{p}_c}$ and $\mathbf{C}_{\mathbf{u}_0}$, the posterior covariance $\tilde{\mathbf{C}}_{\mathbf{u}_0}$ for the estimation of $\mathbf{u}_0$ is (Tarantola 2005, p. 36)

$$\tilde{\mathbf{C}}_{\mathbf{u}_0} = \left(\mathbf{G}^* C_{\mathbf{p}_c}^{-1} \mathbf{G} + C_{\mathbf{u}_0}^{-1}\right)^{-1}$$

Similarly to Grion et al. (1998) and Davison et al. (2011), we use the posterior covariance as a tool to assess the effect of acquisition geometry on inversion result. $\tilde{\mathbf{C}}_{\mathbf{u}_0}$ can be calculated for a range of cable depth profiles and with a calm or rough sea-surface to assess the effect of notch diversity on pre-stack and pre-migration de-ghosting.

For this purpose, we consider a set of cable depth profiles (Figure 1, top) and calculate $\tilde{\mathbf{C}}_{\mathbf{u}_0}$ for the calm and rough sea case in the 0-125Hz band. $\tilde{\mathbf{C}}_{\mathbf{u}_0}$ is calculated assuming that $\mathbf{C}_{\mathbf{u}_0}$ several orders of magnitude larger than $\mathbf{C}_{\mathbf{p}_c}$, and normalized so that a value of 100% corresponds to $\mathbf{C}_{\mathbf{u}_0}$ being equal to $\tilde{\mathbf{C}}_{\mathbf{u}_0}$. In other words, a value of 100% corresponds to de-ghosting failure, as the inversion does not improve the prior state of information. Values smaller than 100% indicate that de-ghosting adds information to the data, with smaller values associated with a smaller amplification of the input noise level. For each frequency, the square roots of the diagonal elements (standard deviations) of $\tilde{\mathbf{C}}_{\mathbf{u}_0}$ are


Figure 1 *De-ghosting posterior standard deviation as a function of frequency and wavenumber. Dark colours indicate small errors; a value of 100 indicates lack of reliability.*

displayed side-by-side in Figure 1. The standard deviations are symmetric with respect to wavenumbers. For convenience, calm and rough sea values are displayed side by side for every cable profile. The rough sea surface used has a 4m significant wave height. It can be noted that in the calm-sea case the perfectly flat cable presents large errors in correspondence to the receiver ghost notch, and that the variations in cable depth of other profiles smoothes the de-ghosting errors. Maximum smoothing is achieved with the strongest cable depth variation. The presence of a rough sea-surface tends to equalize covariance differences for the various cable profiles.

Phase shift de-ghosting example

The following example is from a deep-water Mediterranean setting, acquired in 2015 as part of an acquisition test. A single 3D line with 10km streamers was acquired using two distinct settings for the
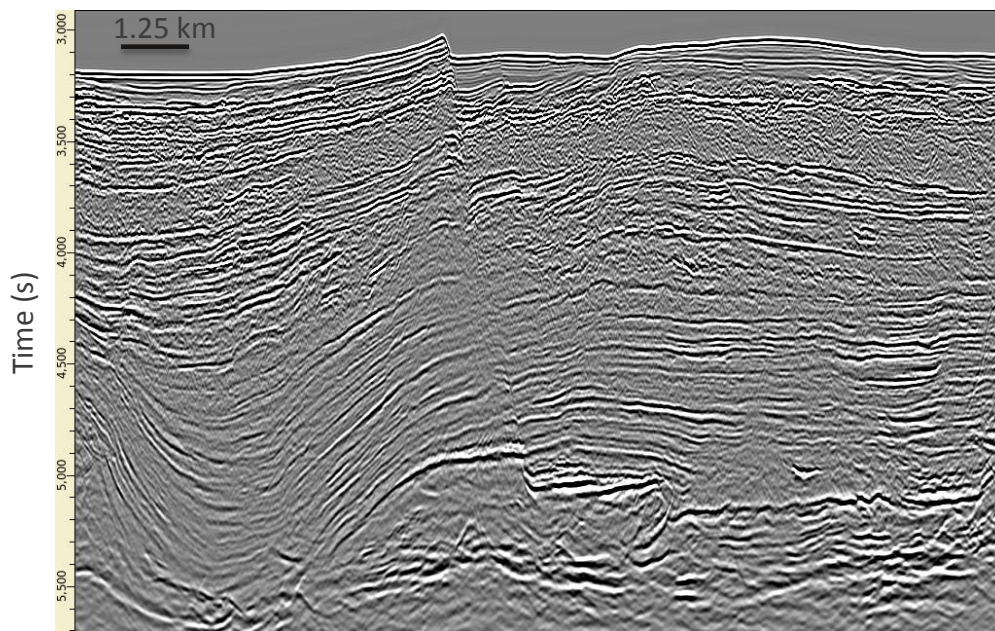
Figure 2 Reference data acquired with a flat, 10m cable depth profile.
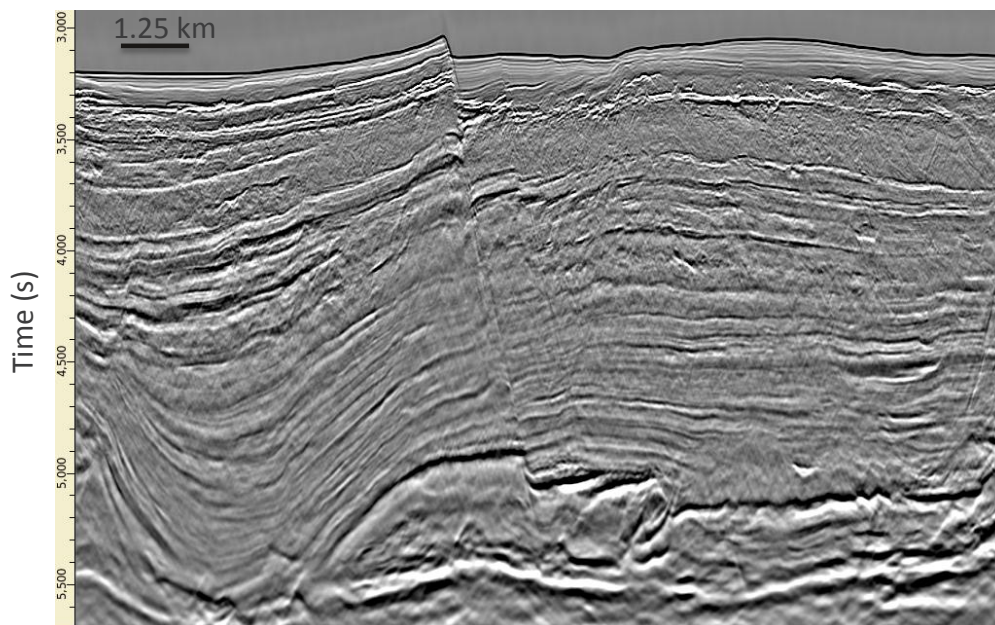
Figure 3 Slanted cable data, with phase-shift de-ghosting applied. Comparison with Figure 2 shows improved continuity and resolution, in particular for the major fault visible at the centre of the image.

central cables: one was flat at 10m and the second slanted from 10m to 20m (a 1m/km slope).

Directional designature, SRME and Kirchhoff time migration were applied to both lines. Near field hydrophone measurements were inverted to estimate directional far field signatures using the procedure outlined in Hargreaves et al., (2015). Directional signature deconvolution was instrumental in getting the correct phase response. If this were inaccurate, spurious side lobes would be apparent, especially at the most reflective interfaces. A PSTM image from the flat cable is in Figure 2 while the slanted cable result is in Figure 3. Only the slanted line had phase-shift receiver de-ghosting applied, and its broader bandwidth has improved the image, especially of the prominent fault in the centre of the section. The prominent black event peaking at around 5000ms is the Top Messinian (a high impedance salt unit) and the strong white event at 5500ms is its base. During the acquisition the weather was good and de-ghosting was carried out under a calm sea assumption. The water velocity was assumed constant: the maximum cable depth was 20m, and a variable water velocity profile is usually relevant for deeper cable configurations.

Conclusions

The up-going wavefield recorded by an arbitrary cable profile and in presence of water velocity variation and a rough sea at mean sea level is estimated by solving a linear system of equations for each frequency of interest. The calculation of the posterior covariance associated with this system provides intuitive insights on the effect of acquisition geometry and sea-state on de-ghosting results. In particular, a rough sea tends to reduce differences induced by cable depth profiles. Application of this de-ghosting method to data acquired with a calm sea and a mildly slanted profile provided satisfactory results.

Acknowledgements

The data shown are provided courtesy of ENI.

References

Davison, C., Ratcliffe, A., Grion, S., Johnston, R., Duque, C., Neep, J., Maharramov, M. [2011] Azimuthal velocity uncertainty: estimation and application. 81st Annual SEG Meeting Expanded Abstracts, 264-268.

Grion, S., Ruffo, P., Rocca, F. [1998] Dispersion of 3D velocity estimators. 60th EAGE Conference, 1-04.

Grion, S., Telling, R., Barnes, J. [2015] De-ghosting by kurtosis maximization in practice, 85th SEG Meeting Expanded Abstracts, 4605-4609.

Hargreaves, N., Grion, S. and Telling, R. [2015] Estimation of air-gun array signatures from near-gun measurements - least-squares inversion, bubble motion and error analysis. 85th SEG Meeting Expanded Abstracts, 149-153.

Hardwick, A., Charron, P., Masoomzadeh, H., Aiyepeku, A., Cox, P. and Laha, S. [2015] Accounting for sea surface evariation in deghosting – a novel approach applied to a 3D dataset offshore west Africa. 85th Annual SEG Meeting Expanded Abstracts, 4615-4619.

King, S. and Poole, G. [2015] Hydrophone-only receiver deghosting using a variable sea surface datum. 85th Annual SEG Meeting Expanded Abstracts, 4610-4614.

Kragh, E., Robertsson, J.O.A., Laws, R., Amundsen, L., Rosten ,T., Davies, T., Zerouk, K., Strudley, A. [2004] Rough-sea deghosting using wave heights derived from low-frequency pressure recordings – a case study. 74th Annual SEG Meeting Expanded Abstracts, 1309-1312.

Paige, C.,C. and Saunders, M. A. [1982], LSQR: An algorithm for sparse linear equations and sparse least squares, ACM transactions on Mathematical Software, Vol. 8, No 1,43-71.

Poole, G. [2013] Pre-migration receiver de-ghosting and re-datuming for variable depth streamer data. 83rd Annual SEG Meeting Expanded Abstracts, 4216-4220.

Riyanti, C.D., van Borselen, R.G., van den Berg, P.M. and Fokkema J. T. [2008] Pressure wave-field deghosting for non-horizontal streamers. 78th Annual SEG Meeting Expanded Abstracts, 2652-2656.

Tarantola, A. [2005] Inverse problem theory, SIAM